Supplementary Material: A Spatially-Lifted SCvx NMPC for Executing SIPP-Generated Time-Corridor Trajectories on an Articulated Loader

Thanh Binh Do and François Guérin

Scope

This document provides the detailed mathematical proofs omitted from the main ECC paper [1], following the same notation and equation numbering. The spatial dynamics are

$$z' = f_a(z, s) + G(z, s)w,$$

with f_a, G as in (13)–(14), admissible state set Z_s defined by Assumption 1, and lifted control set $\mathcal{W}$ by (16). We give constructive proofs for Lemma 1 (well-posedness), Theorem 2 (recursive feasibility with explicit slack bounds), and Theorem 3 (local practical stability).

1 Proof of Lemma 1 (Well-Posedness)

The system

$$f(z, w, s) = f_a(z, s) + G(z, s)w$$

has

$$f_a(z,s) = \begin{bmatrix} (1 - d_f\kappa_{\text{ref}}) \tan e_\theta \\ \dfrac{(1 - d_f\kappa_{\text{ref}}) \sin\gamma}{(L_f \cos\gamma + L_r)\cos e_\theta} - \kappa_{\text{ref}}(s) \\ 0 \\ 0 \\ 0 \end{bmatrix}, \qquad G(z,s) = \begin{bmatrix} 0 & 0 & 0 \\ \dfrac{L_r}{L_f\cos\gamma + L_r} & 0 & 0 \\ 1 & 0 & 0 \\ 0 & 0 & 1 \\ 0 & 1 & 0 \end{bmatrix}.$$

Assumption 1 ensures that all denominators remain bounded away from zero on the compact set Z_s. Define

$$C_w := (1 + \omega_{\max} + a_{\max})\, w_{2,\max}, \quad \text{so that} \quad \|w\| \le C_w \text{ for all } w \in \mathcal{W}.$$

To establish existence and uniqueness, it suffices to show that f is globally Lipschitz in z on Z_s and satisfies Carathéodory's conditions.

Bounded Jacobians. Let $D(\gamma) = L_f \cos\gamma + L_r \geq D_{\min} > 0$. The first component $f_{a,1} = (1 - d_f \kappa_{\text{ref}}) \tan e_\theta$ has derivatives

$$\frac{\partial f_{a,1}}{\partial d_f} = -\kappa_{\text{ref}} \tan e_\theta, \qquad \frac{\partial f_{a,1}}{\partial e_\theta} = (1 - d_f \kappa_{\text{ref}}) \sec^2 e_\theta.$$

Since $|e_\theta| \leq \frac{\pi}{2} - \varepsilon_\theta$, both $\tan e_\theta$ and $\sec e_\theta$ are bounded. Similar arguments applied to

$$f_{a,2} = \frac{(1 - d_f \kappa_{\text{ref}}) \sin\gamma}{D(\gamma) \cos e_\theta} - \kappa_{\text{ref}}(s)$$

show that every partial derivative of f_a remains bounded on Z_s. Thus, there exists $L_a > 0$ such that

$$\left\| \tfrac{\partial f_a}{\partial z}(z, s) \right\| \leq L_a \quad \forall (z, s) \in Z_s \times [0, s_f]. \tag{1}$$

For $G(z, s)$, only $G_{21} = L_r / D(\gamma)$ depends on z, and

$$\frac{\partial G_{21}}{\partial \gamma} = \frac{L_r L_f \sin\gamma}{D(\gamma)^2}$$

is also bounded. Hence there exists $L_G > 0$ such that

$$\left\| \tfrac{\partial g_i}{\partial z}(z, s) \right\| \leq L_G, \quad i = 1, 2, 3. \tag{2}$$

Lipschitz continuity. For any $z_1, z_2 \in Z_s$, $w \in \mathcal{W}$, and $s \in [0, s_f]$,

$$\|f_a(z_1, s) - f_a(z_2, s)\| \leq L_a \|z_1 - z_2\|, \quad \|G(z_1, s)w - G(z_2, s)w\| \leq L_G \|w\| \|z_1 - z_2\|.$$

Therefore,

$$\|f(z_1, w, s) - f(z_2, w, s)\| \leq L \|z_1 - z_2\|, \qquad L := L_a + L_G C_w. \tag{3}$$

Carathéodory conditions. (i) $f(\cdot, w, s)$ is continuous in z since f_a, G are smooth. (ii) $f(z, w, \cdot)$ is measurable because $\kappa_{\text{ref}}(s)$ is measurable. (iii) On the compact domain, $\|f(z, w, s)\| \leq m_{\max}$, so $m(s) \equiv m_{\max}$ is integrable.

Hence, by the Carathéodory theorem [2, 3], the ODE

$$\frac{dz}{ds} = f(z(s), w(s), s), \quad z(0) = z_0,$$

admits a unique absolutely continuous solution for any $z_0 \in Z_s$ and measurable bounded $w(\cdot) \in L^\infty([0, s_f]; \mathcal{W})$, with continuous dependence on $(z_0, w(\cdot))$. This proves Lemma 1. □

2 Proof of Theorem 2 (Recursive Feasibility)

Let $\{(z^\star_{k,j}, w^\star_{k,j})\}$ be the optimal solution of the SCvx subproblem (23) at step k, with nominal $(\bar{z}_j, \bar{w}_j)$. At step $k+1$, the standard shift–append candidate is

$$\tilde{z}_0 = z_{k+1}, \quad \tilde{w}_j = \bar{w}_{j+1}\ (j < N_p - 1), \quad \tilde{w}_{N_p-1} = K_f \tilde{x}_{N_p-1},$$

and the nonlinear update

$$\tilde{z}_{j+1} = \tilde{z}_j + \Delta s\, f(\tilde{z}_j, \tilde{w}_j, s_j).$$

Define $\delta z_j := \tilde{z}_j - \bar{z}_{j+1}$. From (3) and bounded $\|\tilde{w}_j - \bar{w}_{j+1}\| \le \rho_{\max}$,

$$\|\delta z_{j+1}\| \le (1 + L\Delta s)\|\delta z_j\| + C_G \rho_{\max} \Delta s, \tag{4}$$

which yields, via the discrete Grönwall inequality,

$$\|\delta z_j\| \le e^{Lj\Delta s}\|\delta z_0\| + \frac{C_G \rho_{\max}}{L}(e^{Lj\Delta s} - 1).$$

Under $LN_p\Delta s \le 1$, $e^{Lj\Delta s} \le e$, leading to

$$\|\delta z_j\| \le C_z \rho_{\max} N_p \Delta s. \tag{5}$$

For the consistency constraint $\psi(z)$, the Taylor remainder

$$\tilde{\nu}_j = \psi(\tilde{z}_j) - \psi(\bar{z}_j) - \nabla\psi(\bar{z}_j)^\top(\tilde{z}_j - \bar{z}_j) = \tfrac{1}{2}(\tilde{z}_j - \bar{z}_j)^\top \nabla^2\psi(\xi_j)(\tilde{z}_j - \bar{z}_j)$$

satisfies $\|\tilde{\nu}_j\|_\infty \le \frac{1}{2} H_\psi (C_z \rho_{\max} N_p \Delta s)^2 =: \epsilon_\nu$. Thus $\|\nu^\star_j\|_\infty \le \epsilon_\nu$.

The temporal deviation $\delta t_j = \tilde{t}_j - \bar{t}_{j+1}$ follows

$$\delta t_{j+1} = \delta t_j + \Delta s(\tilde{w}_{2,j} - \bar{w}_{2,j+1}),$$

and by Lipschitz continuity of ψ, $|\tilde{w}_{2,j} - \bar{w}_{2,j+1}| \le \tilde{C}\rho_{\max} N_p \Delta s$, leading to

$$|\delta t_j| \le C_\sigma \rho_{\max} N_p^2 \Delta s^2 =: \epsilon_\sigma.$$

Consequently, the time-corridor slacks satisfy $\|\sigma_j^{\pm,\star}\|_\infty \le \epsilon_\sigma$. This establishes the explicit bounds (27)–(29) and recursive feasibility. □

3 Proof of Theorem 3 (Local Practical Stability)

Linearizing the terminal dynamics $(A_{\text{lin}}, B_{\text{lin}})$ and choosing a stabilizing feedback K_f, let P_f solve the Riccati equation with $Q_f \succ 0$. Then for $V(x) = x^\top P_f x$,

$$V(x^+) - V(x) = -x^\top Q_f x$$

in the linear case. For the nonlinear dynamics $x^+ = A_{\mathrm{cl}}x + \phi(x)$ with $\|\phi(x)\| \le c_\phi \|x\|^2$, one obtains

$$V(x^+) - V(x) \le -\lambda_{\min}(Q_f)\|x\|^2 + 2c_A c_\phi \|x\|^3 + c_P c_\phi^2 \|x\|^4.$$

Choosing $r > 0$ such that $2c_A c_\phi r + c_P c_\phi^2 r^2 \le \frac{1}{2}\lambda_{\min}(Q_f)$ ensures

$$V(x^+) - V(x) \le -\tfrac{1}{2}\lambda_{\min}(Q_f)\|x\|^2$$

for $\|x\| \le r$. The terminal set

$$X_f = \{x : x^\top P_f x \le \rho_f\} \subseteq \{x : \|x\| \le r\}$$

thus guarantees invariance and local decrease of V.

For the overall MPC value function V_k, let $(z^\star, w^\star)$ be the optimal solution at step k, $(\tilde{z}, \tilde{w})$ the feasible candidate at step $k+1$. By optimality,

$$V_{k+1} \le J_{\mathrm{nl}}(\tilde{z}, \tilde{w}),$$

and standard MPC arguments yield

$$V_{k+1} - V_k \le -\alpha_3(\|x_k\|) + (\beta_{\mathrm{lin}} + \beta_{\mathrm{slack}})\epsilon,$$

where $\epsilon = \max\{\epsilon_\nu, \epsilon_\sigma\}$,

$$\beta_{\mathrm{lin}} = (N_p L_\ell + L_\Phi) C_z N_p \Delta s, \quad \beta_{\mathrm{slack}} = N_p(\rho_\nu + 2\rho_\sigma).$$

Hence

$$V_{k+1} - V_k \le -\alpha_3(\|x_k\|) + \beta\epsilon, \quad \beta = \beta_{\mathrm{lin}} + \beta_{\mathrm{slack}}.$$

By standard Lyapunov arguments [2, 4], the closed-loop error x_k converges to a neighborhood of the origin of radius $\mathcal{O}(\sqrt{\epsilon})$, establishing local practical stability. □

4 Kinematic Model (Front-Axle-Centric)

4.1 State and Control Inputs

We define the state vector $\mathbf{q}$ based on the pose of the front axle, and the control input vector $\mathbf{u}$ relative to the front axle.

The state vector is:

$$\mathbf{q} = \begin{bmatrix} x_f \\ y_f \\ \theta_f \\ \gamma \end{bmatrix}$$

where (x_f, y_f) is the position of the front axle center, θ_f is the orientation of the front frame, and γ is the articulation angle.

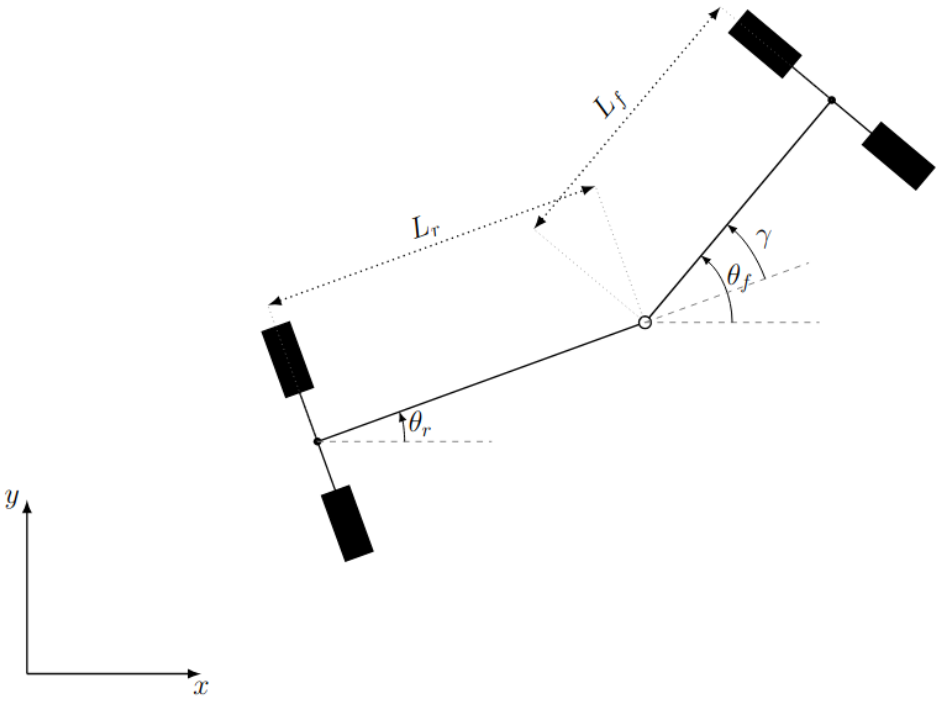

Figure 1: Robot Caterpillar 996

The control input vector is:

$$\mathbf{u} = \begin{bmatrix} v_f \\ \omega_s \end{bmatrix}$$

where v_f is the linear velocity of the front axle and $\omega_s = \dot{\gamma}$ is the articulation (steering) rate.

4.2 Geometric Constraints

The pose of the rear axle is defined algebraically based on the state $\mathbf{q}$. The parameters L_f and L_r are the lengths from the pivot joint to the front and rear axles, respectively.

The rear frame orientation θ_r is:

$$\theta_r = \theta_f - \gamma$$

The rear axle position (x_r, y_r) is reconstructed as:

$$x_r = x_f - L_f \cos(\theta_f) - L_r \cos(\theta_r) \tag{6}$$
$$y_r = y_f - L_f \sin(\theta_f) - L_r \sin(\theta_r) \tag{7}$$

Substituting θ_r, we get the full reconstruction:

$$x_r = x_f - L_f \cos(\theta_f) - L_r \cos(\theta_f - \gamma) \tag{8}$$
$$y_r = y_f - L_f \sin(\theta_f) - L_r \sin(\theta_f - \gamma) \tag{9}$$

4.3 Non-Holonomic (No-Slip) Constraints

4.3.1 Front Axle Constraint

The velocity of the front axle is our control input v_f in the direction θ_f. This directly gives two state derivatives:

$$\dot{x}_f = v_f \cos(\theta_f) \tag{10}$$
$$\dot{y}_f = v_f \sin(\theta_f) \tag{11}$$

4.3.2 Rear Axle Constraint

The velocity of the rear axle $(\dot{x}_r, \dot{y}_r)$ must be in its forward direction θ_r. This side-slip constraint is used to find the rest of the model:

$$\dot{y}_r \cos(\theta_r) - \dot{x}_r \sin(\theta_r) = 0$$

4.4 Derivation of the State-Space Model

We need to find $\dot{\theta}_f$. We take the time derivative of the rear axle position (x_r, y_r) from the reconstruction equations:

$$\dot{x}_r = \dot{x}_f + L_f \sin(\theta_f)\dot{\theta}_f + L_r \sin(\theta_r)(\dot{\theta}_f - \dot{\gamma}) \tag{12}$$
$$\dot{y}_r = \dot{y}_f - L_f \cos(\theta_f)\dot{\theta}_f - L_r \cos(\theta_r)(\dot{\theta}_f - \dot{\gamma}) \tag{13}$$

Substituting these into the rear no-slip constraint yields:

$$\Big(\dot{y}_f - L_f \cos(\theta_f)\dot{\theta}_f - \dots\Big)\cos(\theta_r) - \Big(\dot{x}_f + L_f \sin(\theta_f)\dot{\theta}_f + \dots\Big)\sin(\theta_r) = 0$$

Grouping terms by $\dot{x}_f, \dot{y}_f$, $\dot{\theta}_f$, and $\dot{\gamma}$ simplifies the equation to:

$$(\dot{y}_f \cos\theta_r - \dot{x}_f \sin\theta_r) - \dot{\theta}_f(L_f \cos\gamma + L_r) + L_r\dot{\gamma} = 0$$

Now, substitute the inputs: $\dot{x}_f = v_f \cos\theta_f$, $\dot{y}_f = v_f \sin\theta_f$, and $\dot{\gamma} = \omega_s$. The first term simplifies:

$$v_f \sin(\theta_f)\cos(\theta_r) - v_f \cos(\theta_f)\sin(\theta_r) = v_f \sin(\theta_f - \theta_r) = v_f \sin(\gamma)$$

The full equation becomes:

$$v_f \sin(\gamma) - \dot{\theta}_f(L_f \cos\gamma + L_r) + L_r\omega_s = 0$$

Solving for $\dot{\theta}_f$:

$$\dot{\theta}_f = \frac{v_f \sin(\gamma) + L_r\omega_s}{L_f \cos(\gamma) + L_r}$$

4.5 Final Kinematic Model

The complete front-axle-centric kinematic model is:

$$\dot{\mathbf{q}} = \begin{bmatrix} \dot{x}_f \\ \dot{y}_f \\ \dot{\theta}_f \\ \dot{\gamma} \end{bmatrix} = \begin{bmatrix} v_f \cos(\theta_f) \\ v_f \sin(\theta_f) \\ \frac{v_f \sin(\gamma) + L_r \omega_s}{L_f \cos(\gamma) + L_r} \\ \omega_s \end{bmatrix}$$

5 Extension: Bucket Forward Kinematics

The position of the bucket's center of mass (x_b, y_b) can be found using forward kinematics. This requires adding the bucket angle δ to the state. The top-down projected length of the bucket arm is $L_b \cos(\delta)$.

The position of the bucket is the position of the front axle plus the vector from the axle to the bucket:

$$x_b = x_f + (L_b \cos(\delta)) \cos(\theta_f) \tag{14}$$

$$y_b = y_f + (L_b \cos(\delta)) \sin(\theta_f) \tag{15}$$

Substituting the full expressions for x_f, y_f, and θ_f gives the complete forward kinematics for the bucket:

$$x_b = x_r + L_r \cos(\theta_r) + (L_f + L_b \cos(\delta)) \cos(\theta_r + \gamma) \tag{16}$$

$$y_b = y_r + L_r \sin(\theta_r) + (L_f + L_b \cos(\delta)) \sin(\theta_r + \gamma) \tag{17}$$

References

References

[1] T. B. Do and F. Guérin, "A Spatially-Lifted SCvx NMPC for Executing SIPP-Generated Time-Corridor Trajectories on an Articulated Loader," in *Proc. European Control Conference*, 2026.

[2] H. K. Khalil, *Nonlinear Systems*, 3rd ed. Prentice Hall, 2002.

[3] E. D. Sontag, *Mathematical Control Theory*, 2nd ed. Springer, 1998.

[4] J. B. Rawlings, D. Q. Mayne, and M. Diehl, *Model Predictive Control: Theory, Computation, and Design*, 2nd ed. Nob Hill Publishing, 2017.

[5] Y. Mao *et al.*, "Successive convexification for non-convex optimal control problems and its application to rocket landing," in *AIAA GNC*, 2016.

[6] M. Szmuk, *Successive convexification & high performance feedback control for agile flight*. PhD thesis, 2019.